Luminescence of tetrahedrally coordinated Co^{2+} in zirconia

1993 J. Phys.: Condens. Matter 5 3717

(http://iopscience.iop.org/0953-8984/5/22/023)

J. Phys.: Condens. Matter 5 (1993) 3717–3726. Printed in the UK

Luminescence of tetrahedrally coordinated Co^{2+} in zirconia

V M Orera, R Merino, R Cases and R Alcalá

Instituto de Ciencia de Materiales de Aragón, Universidad de Zaragoza–CSIC, Facultad de Ciencias, 50009 Zaragoza, Spain

Received 29 September 1992, in final form 19 February 1993

Abstract. Co^{2+} enters the lattice of zirconia stabilized with a 46% of yttria in fourfold coordinated cation sites. The absorption spectrum consists mainly of two triplets, one of which is rather weak at around 5500 cm^{-1} (corresponding to the $^4A_2 \rightarrow {}^4T_1(^4F)$ transition), while the other is very intense at around 15 175 cm^{-1} corresponding to the $^4A_2 \rightarrow {}^4T_1(^4P)$ transition. Excitation in the visible region produces two strong broad emission bands at 13 330 and 10 420 cm^{-1} due to the $^4T_1(^4P) \rightarrow {}^4A_2$ and $^4T_1(^4P) \rightarrow {}^4T_2(^4F)$ transitions respectively. The lifetime of the emitting level is $\simeq 0.75$ μs at 10 K. The structure of the triplet states is caused by the combined effect of spin–orbit and Jahn–Teller interactions which, besides the splitting of the cubic levels, produce a strong admixture of some spin doublets with the $^4T_1(^4P)$ level.

We have calculated the energy levels using the Eisenstein matrices thus taking into account both Coulomb, crystal field and spin–orbit interactions. The best fit with the experimental measurements is obtained for the following values of the parameters. $10Dq = 3025$ cm^{-1}, $B = 720$ cm^{-1}, $C/B = 4.0$ and spin–orbit constant $\zeta_{3d} = -515$ cm^{-1}. The $^4T_1(^4P)$ emission suffers a strong thermal quenching at temperatures above 100 K. The evolution with temperature of the intensity of the photoluminescence and its decay curves are discussed with reference to the energy level diagram of the ion and the defective character of the sample.

1. Introduction

The recent success in producing large single crystals of cubic zirconia of a good optical quality opens up new perspectives for their use as an optical material, specifically when reliability under extreme conditions is required.

Yttria-stabilized zirconia (YSZ) has a fluorite structure, the crystal composition being $Zr_{1-x}Y_xO_{2-x/2}$ with x in the range $\simeq 0.1$–0.5. The substitution of Zr^{4+} by Y^{3+} to stabilize the cubic phase results in a high concentration of oxygen vacancies, and from the spectroscopical point of view, YSZ behaviour is between that of a glass and a crystalline material. In practice YSZ can be considered as an anti-glass in a sense that there is short-range disorder at the same time as long-distance order [1]. Thus different lattice sites with a point symmetry lower than cubic will be available for the impurity ions. Since the electronic levels of these ions depend on their environment, large variations of their optical properties with matrix composition are expected.

Consequently, the study of the spectroscopic properties of YSZ doped with ions of the transition series is of current interest, and some efforts have been made previously in spite of the difficulties inherent in using a highly defective material.

The way in which impurity ions enter the zirconia lattice also depends on the kind of ion. For example, we showed that Er^{3+} enters the fluorite-type zirconia lattice in eight and sevenfold coordinated sites at the same time and in a ratio which corresponds with a

0953-8984/93/223717+10$07.50

substitution for the cations at random [2]. Thus the matrix composition determines which impurity configuration will be dominant.

In contrast, 3d ions seem to cluster around them some oxygen vacancies to favour a particular configuration; an example is Cr^{3+} which enters the YSZ lattice in an octahedral site slightly perturbed by the neighbouring defects [3]. This preference for special sites may explain for example the very low solubility of those ions in zirconia compared with the high solubility of some rare-earths.

In the present paper we show that Co^{2+} ions behave in that way and, for example, in $Zr_{0.84}Y_{0.16}O_{1.92}$ they produce the pink colour characteristic of divalent cobalt in an environment of six oxygens whereas the colouration of cobalt doped $Zr_{0.54}Y_{0.46}O_{1.77}$ is blue, which is typical of cobalt in tetrahedral sites [4].

Here we will focus ourselves on the study of the spectroscopical properties of tetrahedrally coordinated cobalt in YSZ. Compared with the octahedral coordination, the absence of inversion symmetry strengthens the transition probabilities in the tetrahedral case and consequently, intense broad absorption and emission bands are expected. That explains the great efforts in searching for systems with tetrahedral d^7 ions, resulting in some examples of well characterized systems involving Co^{2+} in tetrahedral sites. Among them we would like to mention the classical works of Weakliem [5] in several compounds, or in YAG:Co by Wood and Remeika [6] and the more recent works of Abritta and Black [7], Donegan *et al* [8] and Goetz and Schulz [9] in materials with spinel related structures.

In YSZ, a large degree of inhomogeneous broadening in both absorption and emission lines is expected owing to disorder due to the presence of a high concentration of structural oxygen vacancies and substitutional Y^{3+} ions. The absence of sharp lines in the Co^{2+} spectra, makes the analysis of the spectroscopical data difficult which has to be done necessarily to a lesser extent than in non-defective matrices.

2. Experimental procedures

Crystals of $Zr_{0.54}Y_{0.46}O_{1.77}$ doped with 0.15wt.% of Co_3O_4 used in this study were purchased from Ceres Co., USA. The crystals were transparent, blue coloured and with the absorption edge near 300 nm. The refraction index was $n = 2.17$ and the density $\rho \simeq 5.9$ g cm^{-3}.

Optical absorption measurements were made in the 200–2000 nm region using a Hitachi U-3400 spectrophotometer and in the 4000–200 cm^{-1} region in a Perkin–Elmer 883 spectrophotometer. Photoluminescence spectra were obtained by exciting the samples with light either from a 150 W Xe arc-lamp passed through a 0.25 m monochromator, or from He–Ne or argon ion lasers. Fluorescence was detected through a 0.5 m monochromator with a Hamamatsu R-928 photomultiplier for the visible, and Si or Ge detectors for the infrared. The luminescence spectra were corrected from instrumental response using a standard tungsten–halogen lamp calibrated against a National Bureau of Standards lamp. Lifetime measurements were performed, with excitation provided by a tunable dye-laser pulse of $\simeq$ 1 ns and 0.1 nm linewidth and using a Tektronik 2430 digital oscilloscope controlled by a computer. The response of the detection system was faster than 10 ns.

Variable temperatures below 300 K were achieved using a close-cycle cryorefrigerator and with an accuracy of ± 1 K. Above room temperature we used a homemade thermostat where the sample temperature was measured with a precision of ± 5 K.

3. Experimental results and interpretation

3.1. Absorption

In figure 1 we give the optical absorption spectra of the YSZ:Co sample measured at 10 and 300 K. It consists of two well-separated absorption bands, a rather intense one in the visible and the other very weak in the infrared resembling those of tetrahedral Co^{2+} ions in other matrices [5–8]. In figure 1(*a*) we give a schematic energy level diagram for Co^{2+} in a tetrahedral crystal field.

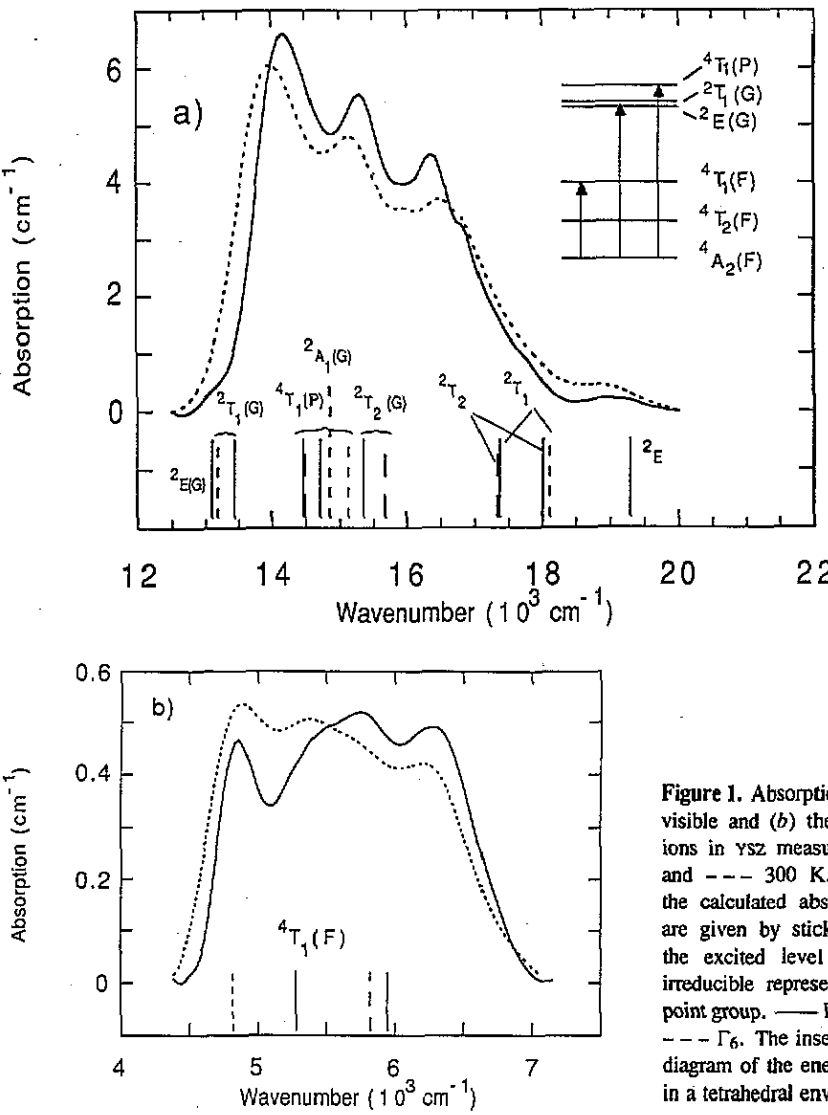

Figure 1. Absorption spectra in (*a*) the visible and (*b*) the infrared of Co^{2+} ions in YSZ measured at 10 K —— and – – – 300 K. The positions of the calculated absorptions (see text) are given by sticks and labelled by the excited level according to the irreducible representations of the T_d point group. —— Γ_8, — — — Γ_7 and – – – Γ_6. The inset gives a schematic diagram of the energy levels of Co^{2+} in a tetrahedral environment.

Within the frame of the crystal field theory we assign the intense triplet at 16 525, 15 175 and 14 000 cm^{-1} (300 K) to the only spin allowed $^4A_2 \rightarrow {}^4T_1(^4P)$ transition in the visible, and the weak one at 6310, 5500 and 4960 cm^{-1} (300 K) to the $^4A_2 \rightarrow {}^4T_1(^4F)$ transition.

The $^4A_2 \rightarrow {}^4T_2(^4F)$ absorption predicted in the $\simeq 3000\ cm^{-1}$ region was not detected. In a pure tetrahedral field this transition is electric dipole forbidden and this may explain its low strength.

Since we do not know the impurity content of our samples we have estimated the oscillator strengths of the absorption bands from the absorption coefficients and measured impurity concentration given in [4] for a crystal of the same composition. Using standard equations (including the local field correction) we have obtained values of $\simeq 1 \times 10^{-3}$ for the $^4A_2 \leftrightarrow {}^4T_1(^4P)$ transition and 4×10^{-5} for the $^4A_2 \leftrightarrow {}^4T_1(^4F)$ transition. These numbers are about 10 times higher than typical values found for Co^{2+} in a centrosymmetric environment and similar to those of tetrahedral Co^{2+} in ZnO [5] supporting our previous hypothesis of a tetrahedral site.

Some shoulders in both the high- and low-energy sides of the visible absorption band are clearly observed and they can be assigned to 'spin forbidden' bands. In particular the shoulder at about $13\,200\ cm^{-1}$ that is more clearly seen in the 10 K spectrum can be assigned to the $^4A_2 \rightarrow {}^2E(^2G) + {}^2T_1(^2G)$ transition, and so the situation will be like that of Co^{2+} in $ZnAl_2O_4$ spinel where the spin doublet also lies below the spin quartet [10].

Another interesting feature of the absorption spectrum given in figure 1(*a*) is the temperature dependence of the visible absorption triplet. We have measured the absorption spectrum as a function of temperature between 10 and 600 K and separated it into its Gaussian components. The area under the absorption band remains essentially constant over all the temperature range but the small changes in the band halfwidths are accompanied by obvious shifts of the peak positions tending to open the triplet as the temperature increases. In figure 2 we give the peak positions versus $\sqrt{T}$. Moreover there is a small asymmetry in the separations between the central peak and the side peaks of the $^4A_2 \rightarrow {}^4T_1(^4P)$ band.

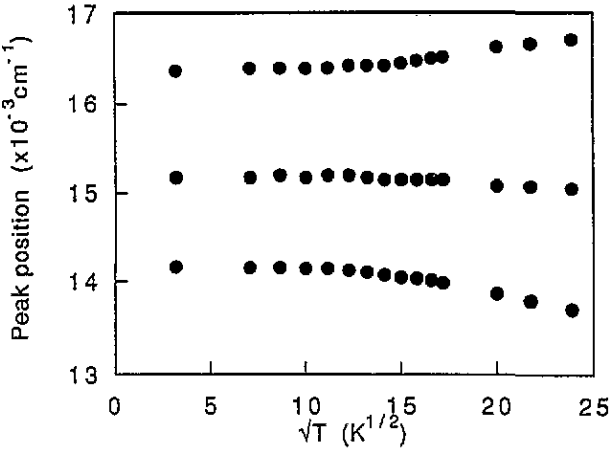

Figure 2. Peak positions of the absorption to the $^4T_1(P)$ level as a function of the square root of temperature.

The temperature dependence of the infrared triplet cannot be so clearly distinguished, in part due to the weakness of the absorption. We did not observe changes in the triplet peak positions comparable to those of the visible band.

3.2. Emission

In figure 3 we show the luminescence spectrum excited at 632 nm with a 0.5 mW He–Ne laser at 77 K. As self-absorption in the high energy side of the emission band can be very

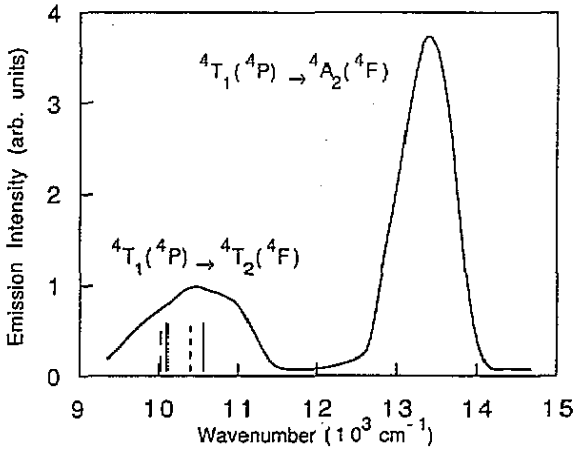

Figure 3. Emission spectrum of Co^{2+} measured at 77 exciting at 632 nm. The sticks labelled as in figure 1 represent theoretical predictions (see text). The spectrum has been corrected for system response.

important we have performed the experiment by exciting with the laser beam tangentially to a polished sample face and detecting at a right angle. The emission consists of two broad bands centred at 13330 and 10420 cm^{-1} which correspond to the $^4T_1(^4P) \rightarrow {}^4A_2(^4F)$ and $^4T_1(^4P) \rightarrow {}^4T_2(^4F)$ transitions respectively (see below). The same emission bands are detected when we excite in other sections of the visible absorption band. The emission band in the IR presents some structure that reflects the splitting of the $^4T_2(^4F)$ level and its halfwidth is about 1500 cm^{-1}. The $^4T_1(^4P) \rightarrow {}^4T_1(^4F)$ emission expected at $\simeq$ 8000 cm^{-1} was not observed.

We have measured the emission bands at temperatures between 10 and 600 K. No vibronic structure was observed in the 10 K measurement. Whereas emission intensities monotonically decrease as the temperature increases only tiny changes either in the peak positions or in the band halfwidths were observed. In figure 4 we give the temperature dependence of their integrated area $\int E\,dE$.

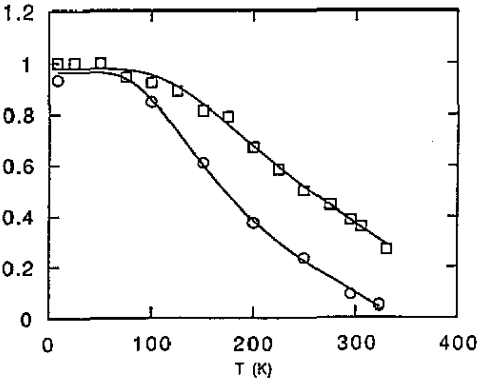

Figure 4. Temperature dependence of the normalized emission decay time (□) and the area under the emission band (○). The lines are only a guide to the eye.

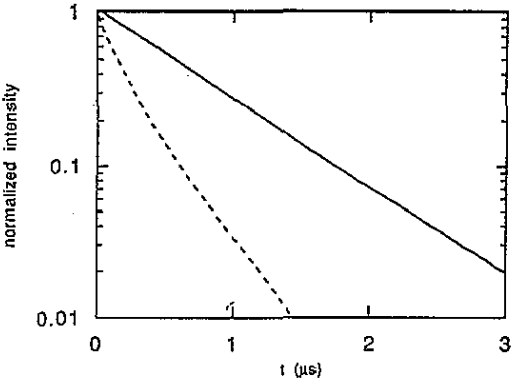

Figure 5. Emission decay curves at two different temperatures: —— 10 K, – – – room temperature.

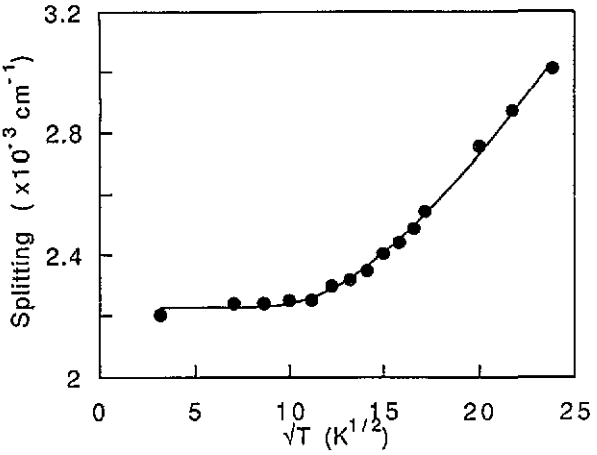

Figure 6. Splittings between the low- and high-energy peaks of the intense absorption band in the visible as a function of the square root of temperature. The line is the fitting using equation (1).

3.3. Emission lifetimes and non-radiative rates

In figure 5 we give the luminescence decays measured at 10 and 300 K with excitation at 640 nm by a laser pulse of $\simeq$ 1 ns and detection at 13 330 cm^{-1}. The dependence of the emission lifetime on temperature is as follows: at 10 K the luminescence decays are well described by a single exponential, the lifetime being 0.75 μs. At higher temperatures the lifetimes shorten, and above $\simeq$ 200 K the decays are clearly non-exponential. Time resolved emission experiments were performed with time gates between 0.01 and 2.00 μs over the whole temperature range. The emission band shapes were the same over the whole time interval.

The lifetime at low temperatures is very short and comparable to that of other Co^{2+} ions in T_d symmetry. For example the lifetime of this level is 0.2 μs in $LiGa_5O_8$ [8] and less than 1 μs in $ZnGa_5O_4$ [7].

Now we can justify our assignment of the emitting level to the $^4T_1(P)$ state rather than to the spin doublets which in the unrelaxed state lie below the spin quartet (see figure 1(*a*)). The short lifetime, the strong emission intensity at low temperatures and the large inhomogeneous broadening and Stokes shift of the emission bands point towards a spin quartet as the emitting level. In fact since the energy of the $^2E(^2G)$ and $^2T_1(^2G)$ spin doublets does not depend very much on the crystal field strength their emission bands should be narrow and with small Stokes shift such as in the case of the R emission in Cr^{3+} [3]. Moreover their lifetimes should be larger than observed. Thus we conclude that in the relaxed configuration of the excited state the bottom of the $^4T_1$ configuration coordinate parabola falls below the spin doublets. This situation is not unusual, an example being the recently studied Cr^{3+} in sillimanite [11].

In figure 4 we plot the effective decay time defined as

$$\tau = \int tI(t)\,dt \Big/ \int I(t)\,dt$$

as a function of temperature. It can be seen that the temperature evolution of the decay time does not follow that of the emission intensity. A similar phenomenon was observed before in octahedral Cr^{3+} but it was in the opposite direction, with the lifetime decreasing faster than the emission intensity as temperature increased [11]. It was explained by a dependence of the radiative transition rate with temperature. Using the same model our results point towards an increase of the radiative time with temperature.

4. Discussion

4.1. Crystal-field levels

Although our experimental results suggest a tetrahedral site for Co^{2+} some deviations from T_d symmetry arising from the defective character of the YSZ matrix are expected. For example a Co^{2+} ion has in its second coordination shell twelve sites that can be occupied in principle at random either by Zr^{4+} or by Y^{3+} ions and a large fraction of empty oxygen sites in the anion sublattice. This imposes a distribution of sites with different crystal field strengths and symmetries which will produce, on the one hand, changes in the positions of those levels depending strongly on the crystal field interaction, and on the other hand, some splitting of the orbitally degenerated states.

Since we failed to perform site resolved spectroscopy and we did not observe any EPR signal that could be associated with Co^{2+} we do not have a direct measure of the strength of those perturbations. Consequently we have to rely on our previous experience in other YSZ systems [3] to tentatively assume that here too the presence of Y^{3+} ions and oxygen vacancies beyond the first coordination shell produces a nearly homogeneous distribution of weak, low symmetry crystal fields that results in a weak perturbation to be added to the stronger tetrahedral field produced by the four nearest oxygen ions.

Based on this argument we perform a crystal field analysis of the spectra assuming a purely tetrahedral symmetry. Crystal-field theory neglects for example the mixing with other ion configurations but it has the advantage of simplicity and has been widely applied to study the low energy d^7 terms.

In T_d symmetry the d^7 ground state is $^4A_2$ and the intense optical absorption bands correspond to the spin allowed transitions to the $^4T_1$ levels. From the centres of these bands and using the matrix elements given by Sugano, Tanabe and Kamimura [12] we get both the Coulomb interaction parameter $B \simeq 720\ cm^{-1}$ and the cubic crystal field strength $10Dq \simeq 3025\ cm^{-1}$. The crystal field strength at the Co^{2+} ion is relatively weak for a cobalt–oxygen distance of $\simeq 2.26$ Å in the undistorted tetrahedra, as compared with other tetrahedral complexes [5]. Here also we can borrow the explanation given by Blasse for a similar effect in Cr^{3+} [1]. The higher charge of the Zr^{4+} and Y^{3+} ions can well favour an outwards relaxation of the oxygen tetrahedra thus producing a weaker crystal field.

The other Racah parameter C can be obtained from the position of the weak spin forbidden absorption band to the $\{^2E + {}^2T_1\}(G)$ levels. It gives $C \simeq 2880\ cm^{-1}$.

With these three parameters we can broadly reproduce the absorption spectrum except for the structure of the spin allowed bands. Several factors can contribute to this structure, for example, the existence of low symmetry perturbations and spin–orbit coupling. If low symmetry fields were the main contribution orbital triplets would split at most into three levels. In the $^4A_2 \rightarrow {}^4T_1(^4F)$ absorption we clearly see four bands (figure 1(*b*)), so some other contributions must be taken into account. Besides, as we have already said we expect a distribution of low symmetry perturbations which will presumably smear out the structure arising from low symmetry fields. So we will study the case in which spin–orbit interaction dominates. Then the ^4T levels split into two Γ_8 and one Γ_6 and Γ_7 states, exactly the four levels we see in figure 1(*b*).

To calculate the effect of the spin–orbit interaction in the optical spectra we have used the matrices describing the spin–orbit interaction given by Eisenstein for a d^3 manifold [13]. We assume that the radial functions of the e and t_2 orbitals do not differ much and therefore the spin–orbit interaction is represented by only one single-electron spin–orbit parameter $\zeta = \zeta'$. Similarly the possible anisotropies in the Racah parameters B and C are neglected and thus we are left with four adjustable interaction parameters B, C, ζ and the cubic crystal

field strength Dq. With these assumptions the Eisenstein matrices reproduce those of the ligand field when $\zeta = 0$.

A spin–orbit constant $\zeta_{3d} = -515\ cm^{-1}$, close to the free ion value of $-535\ cm^{-1}$, was chosen to best fit the structure of the $^4A_2 \rightarrow {}^4T_1(^4F)$ absorption band. Using this value and the parameters given above we have calculated the band positions which are given by sticks in figure 1. It can be seen that besides the structure of the $^4A_2 \rightarrow {}^4T_1(^4F)$ band we can also account for the positions of the weak absorption bands assigned to doublet states at both sides of the intense band in the visible. On the contrary this static model does not explain at all the structure of the intense triplet absorption band in the visible that we have assigned to the intense $^4A_2 \rightarrow {}^4T_1(^4P)$ transition. In fact unreasonable spin–orbit constant values beyond $-1500\ cm^{-1}$ are needed to account for such splitting.

Another test of the fit can be carried out as follows. Although the absorption band corresponding to the $^4A_2 \leftrightarrow {}^4T_2(^4F)$ transition is too weak to be measured, we can estimate the position of the $^4T_1(^4P) \rightarrow {}^4T_2(^4F)$ emission band by subtracting from the energy of the $^4T_1(^4P) \rightarrow {}^4A_2(^4F)$ emission the energies calculated for the $^4T_2(^4F)$ levels. The result is given by sticks in figure 3 and a good fit to the experimental emission band is obtained.

From all these results we conclude that in our crystals Co^{2+} ions are located in the centre of slightly perturbed oxygen tetrahedra and the disorder of the YSZ matrix only contributes to the large inhomogeneous broadening of the bands.

4.2. Jahn–Teller effect

As we have seen above the spin–orbit interaction alone cannot account for all the splitting of the $^4T_1(^4P)$ state. The $^4A_2(^4F) \rightarrow {}^4T_1(^4P)$ absorption band presents a pronounced triple-peaked lineshape and a temperature evolution which are typical features of a dynamical Jahn–Teller (JT) effect which has usually been invoked to explain the structure of the triplet excited states of Co^{2+} [14, 15].

Of course a reasonable treatment of the problem should introduce simultaneously the crystal field, Coulomb, spin–orbit, JT and vibronic interactions in the Hamiltonian describing the system. This is a formidable task that given the absence of any clearly resolved vibronic and zero phonon lines makes this effort unprofitable in our case. In the following we restrict ourselves to a qualitative discussion of the problem and consequently the parameters obtained have to be taken as rough estimates.

The question now is what is the strength of this interaction compared with spin–orbit and which are the predominant coupling vibrational modes. The answer is not clear but a comparison of the measured line shapes with those calculated by Cho [16] suggest to us that JT dominates over the spin–orbit interaction and that $T \otimes \tau$ coupling is also dominant.

In that case and in the frame of a linear JT effect, the splitting between the side and central peaks can be fitted to the expression given by Ulrici [14]:

$$\Delta E(T) = \Delta E_1 + \Delta E(0)[\coth(\hbar\omega/2kT)]^{1/2} \tag{1}$$

where ΔE_1 is the 'static' splitting, $\Delta E(0)$ is related with the coupling constant and ω is the vibrational mode frequency.

The temperature evolution of the splittings given in figure 2 follows indeed equation (1) thus supporting the JT model, but there is an asymmetry between the high- and low-energy splittings and a shift towards the low energies of the central peak which are not predicted by the linear coupling. Quadratic JT coupling can account for these features [15] but even in that case we can use equation (1) to study the temperature evolution of the splitting between the two high and low energy side peaks of the $^4T_1(^4P)$ level after a redefinition of $\Delta E(0)$.

This is done in figure 6 and the data can be fitted to equation (1) with the following parameters: $\Delta E(0) = 1300 \pm 90\ cm^{-1}$, $\Delta E_1 = 900 \pm 85\ cm^{-1}$ and the average interacting vibration mode, $\hbar\omega = 320 \pm 30\ cm^{-1}$. Our samples show a Raman spectrum consisting of a very weak T_{2g} band and a strong phonon density-like band at about $300\ cm^{-1}$ that coincides with the interacting mode deduced from equation (1). The 'static' splitting ΔE_1 is close to that produced by spin–orbit interaction ($\simeq 700\ cm^{-1}$) and from the value of $\Delta E(0)$ we can give an estimate of the JT energy $E_{JT} \simeq 1200 \pm 250\ cm^{-1}$ which is similar to the values found for that band in Co^{2+} doped CaF_2 and CdF_2 ($E_{JT} \simeq 1900\ cm^{-1}$) [14].

In the case of the $^4A_2(^4F) \rightarrow {}^4T_1(^4F)$ band the absence of a triple-peaked lineshape and a temperature evolution as that reported above can be explained because the spin–orbit splitting is in that case dominant.

4.3. Luminescence

Finally we want to discuss the photoluminescence results. We have detected emissions from the lower state of the JT split $^4T_1(P)$ level. The emissions which are very intense at low temperatures, as they should be for spin allowed transitions, show severe thermal quenching at temperatures above 100 K. For 3d ions, the excited states are usually strongly shifted in a configuration coordinate diagram (CCD) with respect to the ground state and the crossing between the excited and the low-lying levels takes place at energies at the bottom of the excited state that can be reached by thermal excitation at moderate temperatures. Then thermal quenching of the luminescence can be explained by a non-radiative process based on the thermal excitation of higher vibrational excited state sublevels above this crossing point.

In the case of tetrahedral Co^{2+} there are some spin doublets close to the low energy JT $^4T_1(P)$ level which are strongly mixed with the spin quartet by both spin–orbit and lattice vibrations. Consequently it is very difficult to propose any reasonable configuration coordinate diagram to account for the emission of the $^4T_1(P)$ state. At this point and based on experimental evidence we can only say that there is a crossing of the potential curves of the excited doublet and quartet that explains why the absorption band to the $^2E(^2G)$ level appears at lower energy than that of the $^4T_1(P)$ level whereas in emission the bottom of the quartet is below the doublet.

The other interesting experimental feature concerns the emission decay curves which are purely exponential at low temperatures but non-exponential at high temperatures. If we neglect the possibility of any energy transfer between cobalt ions because of its low concentration, the non-exponential decays observed at high temperatures can be related with the site distribution in the following way.

As in the case of Cr^{3+} ions in mullite ceramics studied by Wojtowicz and Lempicki [17], we can expect a distribution of the bottom of the potential curves of quartets as well as a spread of shifts in the CCD, due to the defective character of the material. This results in a set of energy differences between the spin quartet and the spin doublet as well as in a distribution of non-radiative rates. Thus at low temperatures when non-radiative probability is low for all the sites the decays are purely radiative and the distribution of decay times narrows.

As the temperature increases, the thermal population of the doublet state can produce the enlargement of the radiative times we have postulated to explain the misfitting between the temperature evolution of the intensity and the decay rates. On the other hand the decay rates are dominated by the non-radiative processes which depend strongly on the ion site thus the distribution of lifetimes becomes broader and non-exponential decays are observed.

Unfortunately, and contrary to the case of Cr^{3+} the thermalized emission from the $^2E(^2G)$ state has not been observed, perhaps because it is under the more intense $^4T_1(P)$ emission and so we are unable to give better experimental support to that model.

Finally and as a conclusion of the present work we can say that our experimental results are clearly in agreement with a slightly perturbed tetrahedral site for Co^{2+}. A comparison of the spectroscopical properties of Co^{2+} in YSZ crystals of different compositions shows the preference of the cobalt ion for tetrahedral sites. In fact for $Zr_{0.84}Y_{0.16}O_{1.92}$ a simple calculation based on a statistically random distribution of oxygen vacancies gives $\simeq 0.5\%$ of octahedral cation sites and a negligible amount (less than 0.01%) of tetrahedral sites. In spite of the small amount of T_d sites available the $^4T_1(^4P) \leftrightarrow {}^4A_2$ emission is clearly detected in this compound. Furthermore the same calculations give in $Zr_{0.54}Y_{0.46}O_{1.77} \simeq 2.5\%$ of O_h and $\simeq 0.1\%$ of T_d sites. Though octahedral sites are plentiful, the absorption spectrum of eightfold coordinated Co^{2+} is not observed. We conclude that divalent cobalt enters the YSZ lattice in special cation sites, either in sites with two oxygen vacancies along a cube diagonal, or preferentially in those having four oxygen vacancies in a tetrahedral array. Such a preference of Co^{2+} for tetrahedral coordination in oxides has been found in many other compounds [5].

Acknowledgment

This work was sponsored by the Dirección General de Investigación Científica y Técnica under contract No PB90-0918.

References

[1] Blasse G 1990 *Mater. Chem. Phys.* **25** 393
[2] Merino R I, Orera V M, Cases R and Chamarro M A 1991 *J. Phys.: Condens. Matter* **3** 8491
[3] Alonso P J, Alcalá R, Casas-Gonzalez J, Cases R and Orera V M 1989 *J. Phys. Chem. Solids* **50** 1185
[4] Aleksandrov V I, Batygov S Kh, Vishnyakova M A, Voron'ko Yu K, Kalabukhova V F, Lavrishchev S V, Lomonova E E, Myzina V A and Osiko V V 1984 *Sov. Phys.–Solid State* **26** 799
[5] Weakliem H A 1962 *J. Chem. Phys.* **36** 2117
[6] Wood D L and Remeika J P 1967 *J. Chem. Phys.* **46** 3595
[7] Abritta T and Black F H 1991 *J. Lumin.* **48, 49** 558
[8] Donegan J F, Anderson F G, Bergin F J, Glynn T J and Imbusch G F 1992 *Phys. Rev.* B **45** 563
[9] Goetz G and Schulz H J 1992 *Phys. Status Solidi* b **169** 217
[10] Ferguson J, Wood D L and van Uitert L G 1969 *J. Chem. Phys.* **51** 2094
[11] Wojtowicz A J and Lempicki A 1989 *Phys. Rev.* B **39** 8695
[12] Sugano S, Tanabe Y and Kamimura H 1970 *Multiples of Transition Metal Ions in Crystals* (New York: Academic)
[13] Eisenstein J C 1961 *J. Chem. Phys.* II **34** 1628
[14] Ulrici W 1984 *The Dynamic Jahn–Teller Effect in Localized Systems. Modern Problems in Condensed Matter Sciences* ed V M Agranovich and A A Maradudin (Amsterdam: North-Holland)
[15] Alonso P J and Alcalá R 1977 *Phys. Status Solidi* **81** 333
[16] Cho K 1968 *J. Phys. Soc. Japan* **25** 1372
[17] Wojtowicz A J and Lempicki A 1988 *J. Lumin.* **39** 189